High-resolution tiled X-ray cone-beam CT using the ASTRA toolbox

Pavel Paramonov[1,2*], Joaquim Sanctorum[1,2*], Domenico Iuso[1,2], Jan Sijbers[1,2], Jan De Beenhouwer[1,2]

[1]imec-Vision Lab, University of Antwerp, Universiteitsplein 1, Building N, Antwerp, B-2610, Belgium,
[2]DynXlab: Center for 4D Quantitative X-ray Imaging and Analysis, Antwerp, 2610, Belgium,
E-mail: pavel.paramonov@uantwerpen.be,

*Joint first authors.

Abstract

Dealing with large and/or elongated objects presents a challenge in micro computed tomography (μCT). In conventional CT, the necessity for the X-ray beam to fully cover the scanned object which has to remain well within the detector boundaries is essential to avoid region-of-interest artifacts in the reconstructed images. Consequently, the magnification of the object and thereby the spatial resolution are limited by the physical dimensions and degrees of freedom of the imaging system. A possible way to increase the magnification and thus the resolution of a μCT image is to perform a tiled scan of the object. In this paper, we propose an iterative reconstruction approach that yields a high-resolution image from such a tiled CT scan. The approach utilizes the ASTRA toolbox, leveraging its key features: the vector-based definition of projection geometry and the linear tomography operators. Our simulations demonstrate that the proposed approach achieves higher resolution through increased magnification.

Keywords: X-ray tomography, micro computed tomography, field of view, iterative reconstruction, cone beam

1 Introduction

X-ray micro computed tomography (μCT) is a powerful inspection tool, with applications that range from biological studies [1] to additive manufacturing [2]. In numerous applications, a cone-beam μCT device is often favored as a balanced choice considering the trade-off between instrumentation cost and scanning speed, in contrast to fan-beam alternatives. Employing a cone-beam configuration allows for enhanced resolution in X-ray CT (XCT) images, achieved by maximizing the magnification factor. However, in scenarios where an image of the entire sample is needed, conventional cone-beam reconstruction techniques, like Feldkamp-Davis-Kress (FDK), impose limitations on the object's achievable magnification. This is because they necessitate the entire object to be fully projected within the detector boundaries. Furthermore, the information for voxels located at a greater distance from the center of rotation (COR) is sampled less densely, which leads to undersampling of the high frequencies in Fourier space and hence position-dependent reconstruction quality.

Several scanning scenarios were proposed to enlarge the effective field of view (FOV) and allow CT with higher magnification. For instance, enlargement of the FOV can be achieved by detector displacement [3, 6], followed by reconstruction of the sample image using either the weighted version of SIRT [4], or with the Wang-FDK method [5]. However, the maximum magnification attainable with these techniques is limited by the requirement that the sample must fit within the cone beam, a constraint that hinders their application in μCT. In [7], the source translation computed tomography (STCT) technique was introduced, where the source is being translated along the trajectory parallel to the detector plane, allowing imaging of elongated objects placed close to the source. To improve angular coverage, STCT can be performed repeatedly at various sample rotation angles, a method referred to by the authors as mSTCT. The sample image can then be reconstructed from mSTCT data using either iterative [7] or analytical methods [8]. Although the authors demonstrated the efficient application of mSTCT in μCT, they also acknowledged a significant increase in acquisition time. Further development of this technique into a full-scan multiple-STCT (F-mSTCT) is presented in [9], along with a dedicated reconstruction algorithm. This new technique reduced the acquisition time but was verified only on 2D data. In [10, 11], 2D XCT geometries with linear and circular arrays of fan beams along with partial reconstruction methods were described and studied. It was shown that the reconstruction methods coupled with circular arrays can be effectively applied in μCT. However, reconstructions from data generated using linear arrays did not yield satisfactory results, as noted in [11].

In this work, we describe an approach for high-resolution, large FOV cone-beam CT using linear arrays. This geometry was selected for its straightforward implementation in laboratory X-ray scanners, like the FleXCT [14], and its capability to achieve the highest possible magnification in CT data. In the proposed method, a series of tomographic scans is conducted with varying sample displacements, where each CT scan referred to as a 'tile'. To reconstruct an XCT image from this tiled CT data, a gradient descent algorithm is employed via the ASTRA toolbox [12]. It is shown that the proposed method demonstrates the ability to reconstruct a large FOV at higher magnification than conventional cone-beam XCT.

2 Methods

The linear array of M projectors is an arrangement of source-detector pairs with a beam displacement distance of $s = 2hd/D$, as shown in Fig. 1a. Each pair yields a partial set of projection images referred to as a 'tile'. By collecting projection data from all

these tiles, artifact-free reconstruction is possible within the radius r_0 [10]:

$$r_0 = M \frac{hd}{\sqrt{D^2 + h^2}} \quad , \tag{1}$$

with d the source-object distance, D the source-detector distance, and h the detector half-width. In this work, the linear array is implemented with a single stationary scanner. The center of rotation (COR) of the sample is translated with the step s along an axis perpendicular to the beam's optical axis, as illustrated in Fig. 1b. Projections over the full angular range are acquired at every lateral position of the sample. The sample is positioned as closely as possible to the X-ray source, dictated by its dimensions and those of the source during rotation. Based on the selected radius of the reconstructed region $\tilde{r}_0 \leq r_0$, the number of required sample positions is determined to be $M = (2N + 1)$, with $N = \left\lceil \tilde{r}_0 \sqrt{D^2 + h^2} \middle/ (2hd) - 1 \right\rceil$ [10].
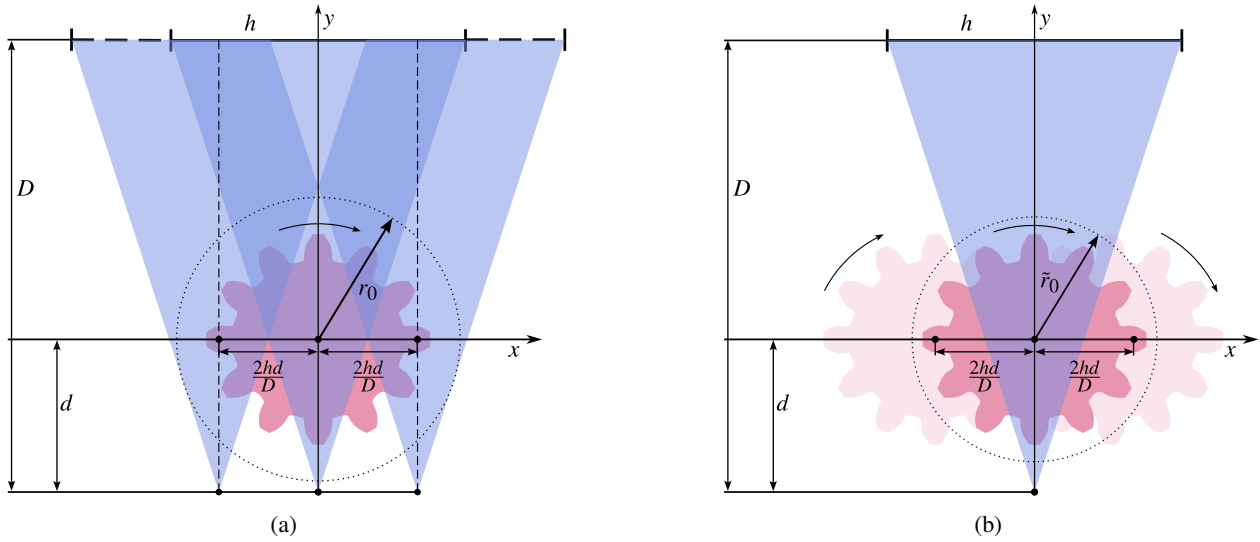

Figure 1: (a) Linear beam array and (b) its equivalent tiled CT geometry. For each sample translation along the x-axis, a CT scan over a full angular range is conducted.

Tiled tomography can be described in an algebraic form:

$$\mathbf{W}\mathbf{b} = \mathbf{p} \quad , \tag{2}$$

with $\mathbf{W}$ the projection matrix, $\mathbf{b}$ the XCT image of the sample, and $\mathbf{p}$ the acquired projections from all tiles. The projection matrix $\mathbf{W}$ is determined by the parameters of the tiled geometry and the dimensions of the image $\mathbf{b}$. The reconstruction of the XCT image $\hat{\mathbf{b}}$ from the tiled data can be done using an iterative method aiming to minimize projection residuals:

$$\hat{\mathbf{b}} = \arg\min_{\mathbf{b}} \|\mathbf{W}\mathbf{b} - \mathbf{p}\|_2^2 \quad . \tag{3}$$

The necessary forward- and back-projection for minimizing Eq. (3) are achieved by utilizing two key features of the ASTRA toolbox: the cone beam vector geometry and the OpTomo operator [12, 13]. The cone beam vector geometry feature enables the specification of individual projection views for the tiled CT, while the OpTomo operator allows for on-the-fly computation of $\mathbf{W}$ and its transpose, thus eliminating the need for memory storage. This method allows for the implementation of iterative reconstruction from the complete set of projection data. Consequently, it eliminates the necessity of stitching together separate reconstructed volumes, thereby streamlining the process and enhancing the accuracy of the final reconstructed image.

3 Experiments

To study the proposed method, we arranged the simulations with the surface mesh of a specially designed resolution phantom shown in Fig. 2a. The simulated sample, a flat disk, has dimensions of 5 mm in thickness and 41 mm in radius. It features circular and rectangular holes, with sizes ranging from 1.0 mm to 62.5 μm. A linear attenuation coefficient of 1.0 was chosen, and all projection simulations and reconstructions were monochromatic. Each experiment simulated a setup achievable in a laboratory X-ray CT system, such as the FleXCT [14].

First, the 3D tiled CT was assessed qualitatively. For this purpose, low-resolution cone-beam tiled projection data was simulated, employing a flat detector comprising 357×357 pixels, each measuring 1.2 mm. The tiled geometry consisted of 3 tiles, with each tile comprising 620 projection angles. The source-detector distance was set at 750 mm, and the source-object distance at
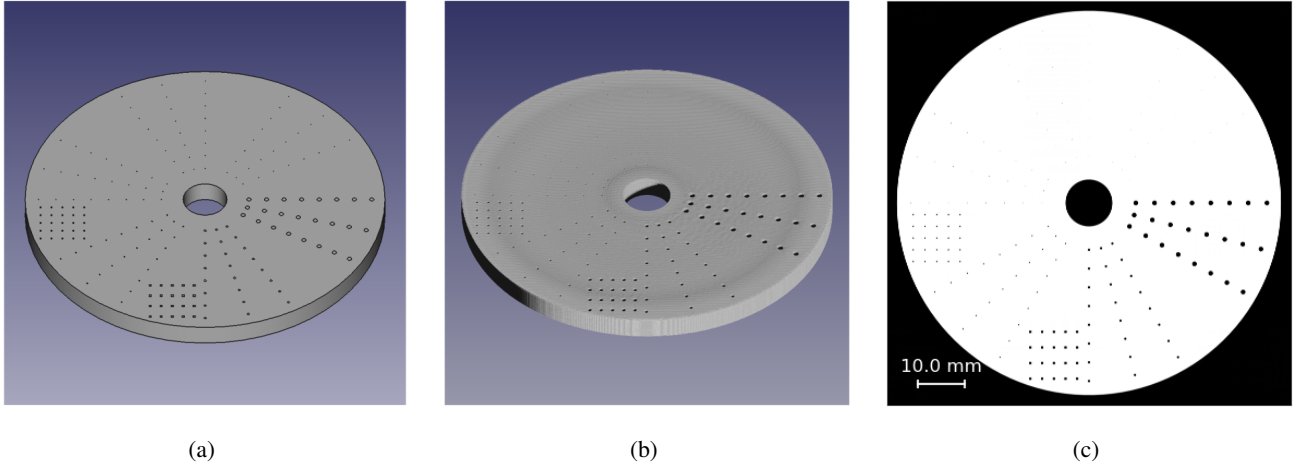
Figure 2: (a) CAD model of the resolution sample, (b) 3D XCT image reconstructed with tiled CT and rendered with the shadowing on, (c) ground truth 2D XCT image of a central slice reconstructed with FBP.

80 mm. A 3D XCT image, as shown in Fig. 2b, was reconstructed using the voxel size of 0.15 mm, employing Barzilai-Borwein (BB) gradient descent [15] for optimization of Eq. (3).

Following this, an experiment was conducted to evaluate the effectiveness of tiled CT in preserving micro-structures within the sample. Parallel-beam projections were initially simulated, followed by the filtered backprojection (FBP) reconstruction of a 2D ground truth XCT image with a voxel size of 12 μm, as illustrated in Fig. 2c. Both full-view and tiled CT high-resolution fan-beam projection data were then simulated. Detailed projection settings for this experiment are presented in Table 1. For the full-view CT data, XCT images were reconstructed using both the FDK algorithm and BB gradient descent optimization of Eq. (3). The XCT image from the tiled data was reconstructed with BB gradient descent optimization of Eq. (3). To ensure a reliable comparative analysis, all images were reconstructed with a consistent voxel size of 12 μm, determined by the magnification inherent in the tiled geometry.

Table 1: Parameters of high-resolution 2D full-view and tiled CT.

Parameter	Value	
	Full-view CT	Tiled CT
Source-detector distance D (mm)	750	750
Source-object distance d (mm)	220	75
Magnification	3.41	10
Total number of projections	4100	12300
Number of tiles M	1	3
Detector size $2h$ (mm)	428.40	428.40
Detector rows	1	1
Detector columns	2856	2856
Detector pixel size (mm)	0.15	0.15
Radius of reconstructed region $\tilde{r}_0$ (mm)	60.42	60.42
Voxel size (μm)	12	12

4 Results and discussion

The resolution capabilities of both conventional and tiled CT are illustrated in Fig. 3, where zoomed-in XCT images are displayed. In Figs. 3a-d, the focus is on the rectangular hole located at the bottom part of the sample, which measures 500 μm. It can be observed that the tiled reconstruction yields sharper details compared to the conventional full-view CT, when reconstructed with either FDK or BB gradient descent methods. Enhanced sharpness of edges is also visible in the 1D intensity plot presented in Fig. 4a, which is plotted along profile A, as shown in Figs. 3a-d. The examination of detail retention relative to the voxel distance from COR is demonstrated by the circular holes in the upper part of the sample. Each hole, measuring 90 μm, is shown in Figs. 3e-l. The hole displayed in Figs. 3e-h is positioned 10 mm from the COR, whereas the hole in Figs. 3i-l is 38 mm from the COR. Although the edges of these holes appear nearly identical in the images reconstructed from conventional CT data, they are sharper in those acquired with the tiled CT, particularly for the peripheral hole. This is clearly depicted in Figs. 4b-c, where 1D radial profiles along the lines B and $\hat{B}$ from Figs. 3e-l are exhibited for all XCT images.
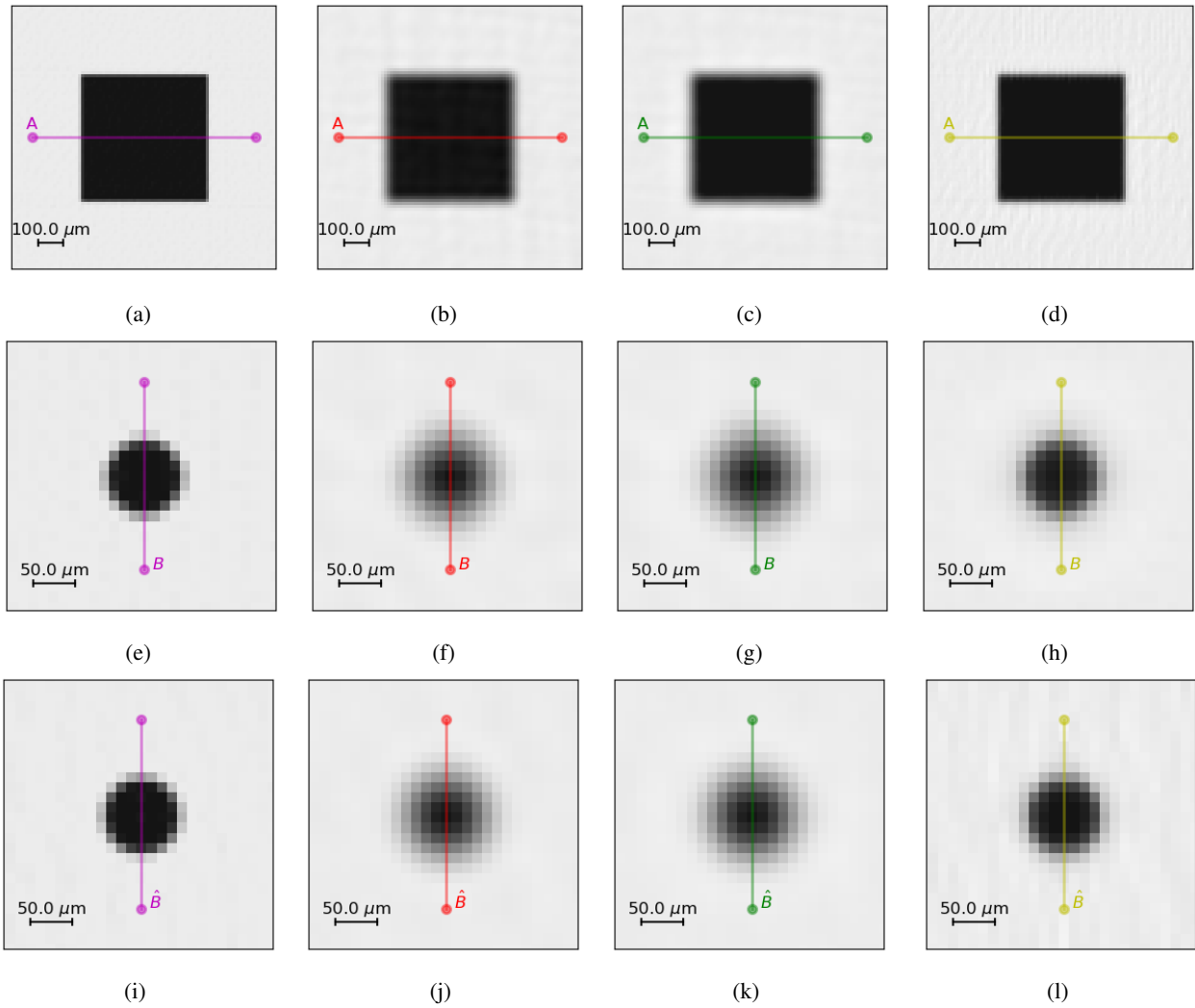
Figure 3: Zoomed-in high-resolution 2D XCT images. First column: ground truth; second column: full-view CT reconstructed with the FDK algorithm; third column: full-view CT reconstructed with the BB gradient descent; fourth column: tiled CT reconstructed with BB gradient descent.
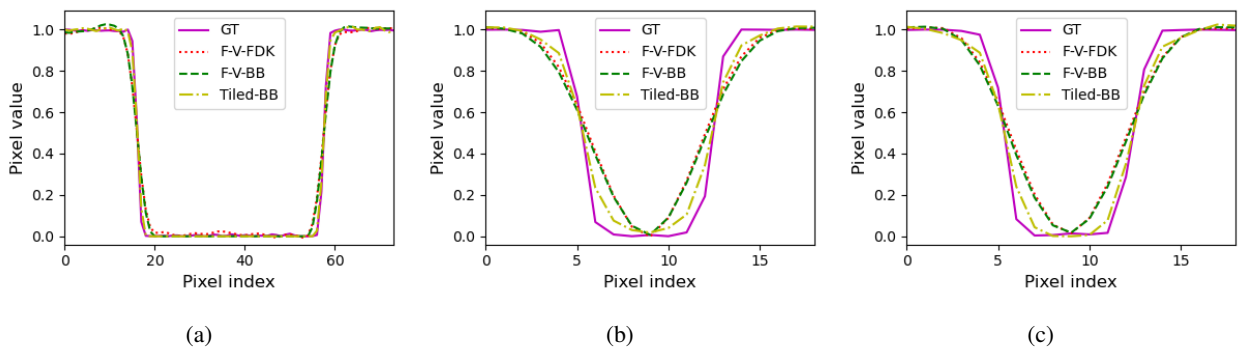

Figure 4: Intensity profiles along the lines (a) A, (b) B, and (c) $\hat{B}$, as shown in Fig. 3. "GT" corresponds to the ground truth, "F-V-FDK" to the full-view FDK reconstruction, "F-V-BB" to the full-view BB reconstruction, and "T-BB" to the tiled BB reconstruction.

5 Conclusion

In this paper, an approach to high resolution, large-field-of-view cone-beam CT based on reconstruction from tiled cone beam data using the vector geometry of the ASTRA toolbox was presented. The findings of the study indicate that this proposed approach enables the resolution of micro-details due to higher magnification for the region of interest that encompasses the

entire object. When compared to conventional cone-beam CT, it was observed that tiled CT is more effective in retaining these micro-structures. Future work will be directed along several paths. First, consideration will be given to the impact of source spot size and projection noise, which typically affect system resolution. Second, optimization of the tiled geometry will be pursued, aiming to reduce the number of projection angles required. Third, the robustness of the actual tiled acquisition process will be examined in relation to the accuracy of COR value estimation, a factor known to impact the quality of reconstruction.

Acknowledgements

References

[1] A. du Plessis, C. Broeckhoven, A. Guelpa, S. Gerhard le Roux, Laboratory x-ray micro-computed tomography: a user guideline for biological samples, GigaScience 6 (2017) gix027

[2] A. Du Plessis , I. Yadroitsev, I. Yadroitsava, S.G. Le Roux, X-Ray microcomputed tomography in additive manufacturing: a review of the current technology and applications, 3D Print. Addit. Manuf. 5 (2018) 227 - 247.

[3] J.G. Sanctorum, S. Van Wassenbergh, V. Nguyen, J. De Beenhouwer, J. Sijbers, J.J.J. Dirckx, Extended imaging volume in cone-beam x-ray tomography using the weighted simultaneous iterative reconstruction technique, Phys. Med. Biol. 66 (2021) art. no. 165008.

[4] J. Gregor, T. Benson, Computational analysis and improvement of SIRT, IEEE Trans. Med. Imaging. 27 (2008) 918-924.

[5] Wang, G., X-ray micro-CT with a displaced detector array, Med. Phys. 29 (2002) 1634-1636.

[6] Q. Lin, M. Yang, Q. Wu, B. Tang and X. Zhang, A reconstruction method through projection data conversion under the displaced detector scanning for industrial cone-beam CT, IEEE Trans. Nucl. Sci. 66 (2019) 2364-2378.

[7] H. Yu, L. Li, C. Tan, F. Liu, R. Zhou, X-ray source translation based computed tomography (STCT), Opt. Express 29 (2021) 19473 - 19758.

[8] H. Yu, S. Ni, J. Chen, W. Ge, L. Zhang, F. Liu, Analytical reconstruction algorithm for multiple source-translation computed tomography (mSTCT), Appl. Math. Model. 117 (2023) 251-266.

[9] J. Chen, H. Yu, S. Ni, C. Liu, W. Ge, Y. Huang, F. Liu, Weighted filtered back-projection for source translation computed tomography reconstruction, IEEE Trans. Instrum. Meas. 72 (2023) 1-9.

[10] M. Müller, G.R. Arce, R.A. Blake, Synthetic scanner arrays in tomographic reconstructions from fan- and cone-beam projections, Appl. Opt. 33 (1994) 8255 - 8269.

[11] M. Müller, G.R. Arce, Generalized fan beam reconstruction algorithm and its applications, J. Opt. Soc. Am. A. 11 (1994) 2410.

[12] W. van Aarle, W.J. Palenstijn, J. Cant, E. Janssens, F. Bleichrodt, A. Dabravolski, J. De Beenhouwer, K.J. Batenburg, J. Sijbers, Fast and flexible X-ray tomography using the ASTRA Toolbox, Opt. Express 24 (2016) 25129 - 25147.

[13] F. Bleichrodt, T. van Leeuwen, W.J. Palenstijn, W. van Aarle, J. Sijbers, K.J. Batenburg, Easy implementation of advanced tomography algorithms using the ASTRA toolbox with Spot operators, Numer. Algorithms 71 (2016) 673 - 697.

[14] B. De Samber, J. Renders, T. Elberfeld, Y. Maris, J. Sanctorum, N. Six, Z. Liang, J. De Beenhouwer, J. Sijbers, FleXCT: a flexible X-ray CT scanner with 10 degrees of freedom, Opt. Express 29 (2021) 3438-3457

[15] J. Barzilai, J. M. Borwein, Two-point step size gradient methods, IMA J. Numer. Anal. 8 (1988) 141-148.